AI-Driven Design of a Quasi-digitally-coded Wideband Microstrip Patch Antenna Array

Mobayode O. Akinsolu*, Yasir I. A. Al-Yasir†, Qiang Hua‡, Chan See§, Bo Liu**

*Faculty of Arts, Science and Technology, Wrexham University, U.K., m.o.akinsolu@ieee.org
†Faculty of Engineering and Informatics, University of Bradford, U.K., alyasir442@gmail.com
‡School of Computing and Engineering, University of Huddersfield, U.K., q.hua@hud.ac.uk
§School of Computing Engineering and the Built Environment, Edinburgh Napier University, U.K., c.see@napier.ac.uk
**James Watt School of Engineering, University of Glasgow, U.K., bo.liu@glasgow.ac.uk

Abstract—Artificial intelligence (AI) is enabling the automated design of contemporary antennas for numerous applications. Specifically, the use of machine learning (ML)-assisted global optimization techniques for the efficient design of modern antennas is now fast becoming a popular method. In this work, we demonstrate for the first time, the ML-assisted global optimization of a high-dimensional non-uniform overlapping quasi-digitally coded microstrip patch antenna array using a new AI-driven antenna design technique, called TR-SADEA (the training cost-reduced surrogate model-assisted hybrid differential evolution for complex antenna optimization). The TR-SADEA-generated array showed very promising simulated frequency responses for potential wideband applications with a -10 dB impedance bandwidth of 5.75 GHz to 10 GHz, a minimum in-band realized gain of 5.82 dBi, and a minimum in-band total radiation efficiency of 87.84%.

Index Terms—AI, Antenna Optimization, and TR-SADEA.

I. INTRODUCTION

The automatic design of antennas via artificial intelligence (AI) techniques in the form of machine learning (ML)-assisted optimization is attracting much attention. This growing interest can attributed to the reduced design time and higher design solution quality that ML-based optimization methods for antenna design offer [1]. This is as opposed to traditional experience-driven methodologies that often rely on parameter sweeping and/or the use of rules of thumb [2]. Even though parameter sweeping and some rules of thumb allow designers to gain insights into the characteristics of antennas, they are often not suitable for the efficient tuning of present-day antenna structures that have interrelated design parameters. As a result, finding the best set of parametric values for modern antennas to meet stringent specifications in terms of bandwidth (e.g., wideband and multiband), radiation and other frequency responses often requires an optimization procedure [3], [4].

AI-based methods available for antenna optimization today often work by incorporating ML techniques into the optimization kernel of traditional numerical optimization methods [1], [5], [6]. This is mostly to address the drawbacks of conventional numerical optimization methods [4]. For example in [7], trust region gradient-based search co-working with the sequential quadratic approximation algorithm has been used to optimize an antenna for gain enhancement using an initial design provided by the designer as the anchor point for the optimization process. However, for antenna design cases where good initial designs are unavailable, other approaches such as the harmonious working of supervised learning and evolutionary computation techniques can be employed as carried out in [8] for the design of a frequency re-configurable antenna array. These examples and several others (such as [9]–[11]) realistically demonstrate how AI, specifically, ML, is automating the antenna design process.

Some ML-based methods for antenna optimization also have their limitations, e.g., not being able to handle more than a few design parameters, and reliance on good initial designs [4]. Due to the increasing complexity of antenna structures to meet stringent design specifications and functional requirements for present-day and future applications, contemporary antenna design problems may have over 40 critical design parameters without a good initial design [12]. For such cases, designers are typically compelled to use design experience to reduce the number of the design parameters to be tuned prior to the ML-driven optimization process to reduce computational cost [12]. However, it will be more efficient to employ a method (such as the training cost-reduced surrogate model-assisted hybrid differential evolution for complex antenna optimization (TR-SADEA) [13]) that can naturally optimize high-dimensional antenna structures without relying on a good initial design.

The TR-SADEA method belongs to the SADEA family of algorithms [14]. It mainly comprises a self-adaptive Gaussian process (GP)-based surrogate modeling method that cuts the training time and speeds up convergence, while mostly maintaining the accuracy of the antenna performance prediction, and a new hybrid surrogate model-assisted antenna optimization framework [13]. In this work, the TR-SADEA method is employed to provide a methodology for the global optimization of a high-dimensional quasi-digitally coded microstrip patch antenna array for wideband applications. It is the first time that the automated design of such a high-dimensional array using TR-SADEA is being presented. Hence, the primary contribution of this work is the TR-SADEA-driven design methodology for such a high-dimensional quasi-digitally coded antenna. Even though there are several approaches available for the digital coding of antennas for both design and performance enhancements [15]–[17], the quasi-digital coding scheme via geometric manipulations presented in [17]

has been adopted in this work due to its straightforwardness. Hence, a design that stems from the work in [17] is the reference design in this paper.

II. ANTENNA GEOMETRY

A primitive layout of the array is shown in Figs. 1 and 2, and its original frequency responses in terms of reflection coefficient and radiation properties for different configurations are discussed in [17]. From Figs. 1 and 2, it can be seen that the antenna geometry is made up of four layers: the full ground plane, the air gap, the dielectric substrate, and the microstrip patch array. The ground plane and array are made of copper having a thickness of 0.03 mm, the dielectric substrate has an initial thickness (h_1) of 0.8 mm, an initial relative permittivity (ϵ_r) of 3.2 and a loss tangent ($\tan(\delta)$) of 0.0033. The air gap between the ground plane and dielectric layer has a thickness (h_2) of 8 mm. The antenna structure is fed using a non-planar coaxial probe connector, and it has been modeled and discretized in CST Studio Suite (CST) using a mesh density of 12 cells per wavelength to have about 303,000 mesh cells in total.

To quasi-digitally code the antenna structure for a non-uniform overlapping topological evolution of its microstrip patch array, the relative positions of the individual cells or patches are coded in CST to allow for their free movement or shifting along the Y-axis as shown in Fig. 1. This quasi-digital coding of the relative positioning of the patches via parametrization in CST allows for an efficient way to determine the best non-uniform overlapping arrangement of the cells as exemplified in [17]. In [17], a genetic algorithm (GA) has been used for the optimization of the array to have different topologies, and the largest -10 dB impedance bandwidth reported is 760 MHz. In this work, we aim to provide a more efficient methodology for finding the best non-uniform overlapping arrangement for the array cells to have the largest possible -10 dB impedance bandwidth in the ultrawideband (UWB) frequency spectrum of 3.1 GHz to 10.6 GHz) with good in-band radiation properties. To achieve this, TR-SADEA is employed to optimize a reference design inspired by the work in [17].

III. TR-SADEA-BASED OPTIMIZATION

The adopted design methodology is shown in Fig. 3. The first step involves the parametrization and quasi-digital coding of the array in CST. This is implemented by defining a Y-axis translation vector for each of the 56 cells of the array to have a total of 56 parameters (i.e., $m1$ to m_{77} in Fig. 1). Aside from the 56 design parameters associated with the relative positioning of the cells, other critical design parameters identified include the position of the feed probe connector (i.e., the ordered pair, (F_X,F_Y), h_1 and ϵ_r. The dimensions of each cell, i.e., the length (P_L) and the width (P_W) are fixed at 7 mm as recommended in [17]. By including the relative position of the feed probe connector in the optimization process, the possibility of obtaining the desired -10 dB wideband

TABLE I: Search Space for the Antenna Design Parameters and their Optimal Values Obtained by TR-SADEA. All Parameters are Continuous Variables with Dimensions in mm, except h_1 and ϵ_r which take values in {0.2, 0.3, 0.4, 0.5, 0.8, 1.5, 2.3, 3, 3.8} and {2.33, 2.5, 3.0, 3.38, 3.5, 4.5, 6.15, 10.2}, respectively.

Design Parameters and their Search Ranges	TR-SADEA Optimum
$m1$ [0 to 56]	40.51
$m12$ [0 to 56]	28.05
$m13$ [0 to 56]	30.92
$m14$ [0 to 56]	36.83
$m15$ [0 to 56]	43.86
$m16$ [0 to 56]	3.96
$m17$ [0 to 56]	10.89
$m2$ [0 to 56]	18.18
$m21$ [0 to 56]	17.86
$m22$ [0 to 56]	34.17
$m23$ [0 to 56]	27.64
$m24$ [0 to 56]	15.43
$m25$ [0 to 56]	27.87
$m26$ [0 to 56]	12.72
$m27$ [0 to 56]	23.69
$m3$ [0 to 56]	29.98
$m31$ [0 to 56]	44.67
$m32$ [0 to 56]	9.81
$m33$ [0 to 56]	4.96
$m34$ [0 to 56]	16.18
$m35$ [0 to 56]	39.72
$m36$ [0 to 56]	4.34
$m37$ [0 to 56]	37.35
$m4$ [0 to 56]	8.63
$m41$ [0 to 56]	12.16
$m42$ [0 to 56]	26.04
$m43$ [0 to 56]	7.30
$m44$ [0 to 56]	18.76
$m45$ [0 to 56]	0.34
$m46$ [0 to 56]	25.21
$m47$ [0 to 56]	32.96
$m5$ [0 to 56]	44.00
$m51$ [0 to 56]	28.62
$m52$ [0 to 56]	23.69
$m53$ [0 to 56]	4.91
$m54$ [0 to 56]	29.72
$m55$ [0 to 56]	25.53
$m56$ [0 to 56]	20.69
$m57$ [0 to 56]	1.53
$m6$ [0 to 56]	26.88
$m61$ [0 to 56]	12.63
$m62$ [0 to 56]	24.96
$m63$ [0 to 56]	16.77
$m64$ [0 to 56]	23.29
$m65$ [0 to 56]	11.52
$m66$ [0 to 56]	29.22
$m67$ [0 to 56]	1.56
$m7$ [0 to 56]	7.06
$m71$ [0 to 56]	49.97
$m72$ [0 to 56]	49.09
$m73$ [0 to 56]	48.25
$m74$ [0 to 56]	4.79
$m75$ [0 to 56]	35.78
$m76$ [0 to 56]	46.19
$m77$ [0 to 56]	44.47
F_X [4 to 10]	6.48
F_Y [-16 to -10]	-11.63
P_W [Fixed]	7.00
P_L [Fixed]	7.00
h_1 {0.2, 0.3, 0.4, 0.5, 0.8, 1.5, 2.3, 3, 3.8}	0.20
ϵ_r {2.33, 2.5, 3.0, 3.38, 3.5, 4.5, 6.15, 10.2}	3.50
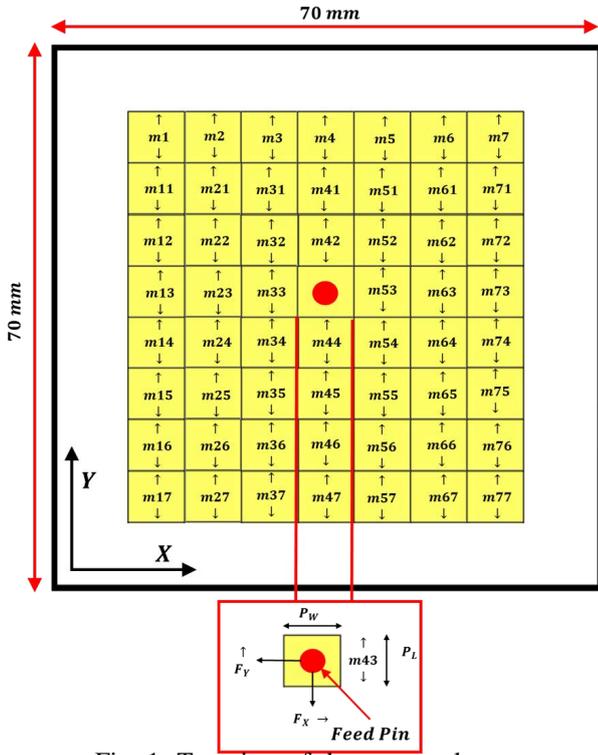
Fig. 1: Top view of the antenna layout.
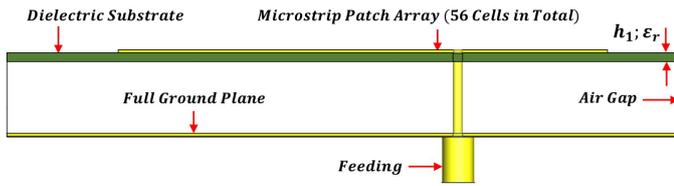
Fig. 2: Side view of the antenna layout.
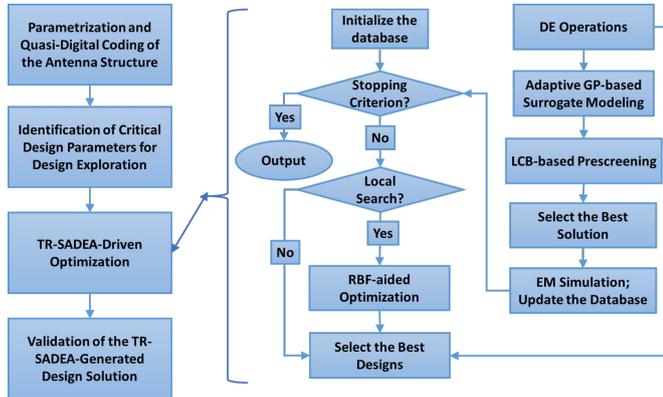
Fig. 3: Proposed methodology and TR-SADEA flow diagram.

impedance matching either via contacting feeding or non-contacting (proximity-coupled) feeding is enabled.

The design parameters identified for the design exploration are shown in Table I and described in Figs. 1 and 2. Using a population size of 250 (all other algorithmic parameters have the default settings in [13]), the TR-SADEA-driven

optimization is initialized by sampling the design space of the array. The initial database comprising the candidate designs and their simulation results is then created. The best candidate design solution is outputted from the database if the preset stopping criterion (maximum number of electromagnetic (EM) simulations) is satisfied; otherwise, TR-SADEA executes the following sequential steps iteratively: (1) Determination of whether local optimization should be used. If yes, implementation of radial basis function (RBF)-assisted local optimization using the current best design as the starting point. Then update of the current best design if a better design solution is found or when necessary. (2) Application of differential evolution (DE) operations to the formulated population to have new child solutions. (3) Self-adaptive GP-based surrogate modeling. (4) Estimation of the DE-generated child solutions using the GP-based surrogate models and the lower confidence bound-based prescreening. (5) Simulation of the estimated best child solution and updating the database with the best child solution and its simulation results. The efficiency improvement of TR-SADEA stems from the use of RBF-assisted local optimization and self-adaptive GP surrogate modeling methods [13]. More details about the TR-SADEA method can be found in [13].

The goal of the TR-SADEA-driven optimization is finding the largest possible -10 dB impedance bandwidth percentage (BW) in the UWB frequency spectrum of 3.1 GHz to 10.6 GHz subject to a minimum in-band realized gain (G_{min}) better than 3 dBi and a minimum in-band total radiation efficiency (η_T) better than 60%. To achieve this goal, the penalized cost function (F) is minimized by TR-SADEA:

$$F = -BW + w \times \{max([3\ dBi - G_{min},\ 0]) + \ldots \\ max([60\% - \eta_T,\ 0])\} \quad (1)$$

with w=50 to make TR-SADEA preferentially focus on meeting the G_{min} and η_T requirements first, before maximizing BW.

After 1,222 EM simulations (costing about 10 days), TR-SADEA obtained a design with $F = -56.6\%$ using a computing budget of 1,500 EM simulations. This design is reported in Table I and its layout is shown in Fig. 4a where it can be seen that its impedance matching is via proximity EM-coupling (such non-contact feeding via proximity coupling is a known concept [18]). The frequency responses for this design solution are shown and compared to the reference design in Figs. 4b, 4c, and 4d. From Figs. 4b, 4c, and 4d, it can be seen that the TR-SADEA-generated design shows better frequency responses in the band of interest in comparison to the reference design. Specifically, the TR-SADEA-generated design has a wide -10 dB impedance bandwidth (5.75 GHz to 10 GHz), a minimum in-band realized gain of 5.82 dBi, and a minimum in-band total radiation efficiency of 87.84%.

IV. CONCLUSION

In this work, a high-dimensional non-uniform overlapping microstrip patch antenna array for wideband applications is
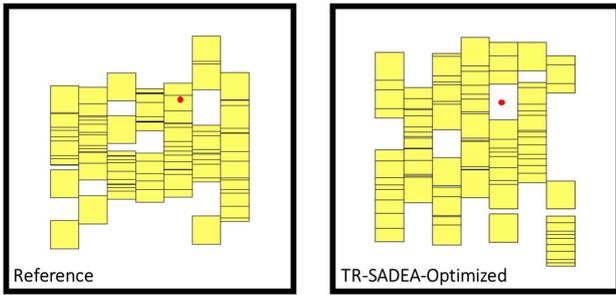
(a) Topological arrangement of the cells of the array.
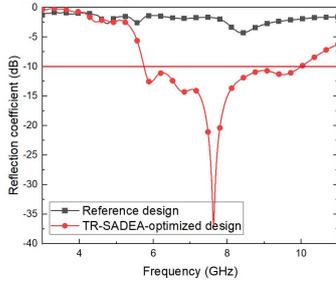
(b) Reflection coefficient.
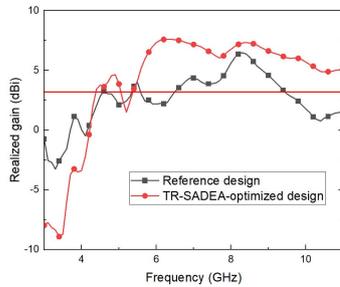
(c) Realized gain.
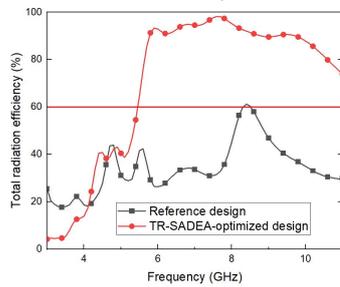
(d) Total radiation efficiency.

Fig. 4: Topological arrangement and simulated results for the reference design and the TR-SADEA-optimized design.

proposed. Thanks to the TR-SADEA-driven optimization approach employed to optimize the reference design for the array, the proposed array offers a wide -10 dB impedance matching over the frequency bandwidth of 5.75 GHz to 10 GHz, a minimum in-band realized gain of 5.82 dBi and a minimum in-band total radiation efficiency of 87.84%. The simulated frequency responses of the TR-SADEA-generated array validate the TR-SADEA method's ability to efficiently handle the optimization of high-dimensional antenna array design problems. In the future, the proposed array will be further

investigated for prototyping or physical implementation.

REFERENCES

[1] Q. Wu *et al.*, "Machine-learning-assisted optimization and its application to antenna designs: Opportunities and challenges," *China Communications*, vol. 17, no. 4, pp. 152–164, 2020.
[2] F. T. Çelik, S. Joof, and K. Karaçuha, "A dual-polarized bandwidth enhanced filtering dipole antenna design for 5g," *IEEE Access*, vol. 11, pp. 78 754–78 767, 2023.
[3] S. Koziel and A. Pietrenko-Dabrowska, "Improved-efficacy em-driven optimization of antenna structures using adaptive design specifications and variable-resolution models," *IEEE Transactions on Antennas and Propagation*, vol. 71, no. 2, pp. 1863–1874, 2023.
[4] V. Grout *et al.*, "Software solutions for antenna design exploration: A comparison of packages, tools, techniques, and algorithms for various design challenges," *IEEE Antennas and Propagation Magazine*, vol. 61, no. 3, pp. 48–59, 2019.
[5] H. M. El Misilmani *et al.*, "A review on the design and optimization of antennas using machine learning algorithms and techniques," *International Journal of RF and Microwave Computer-Aided Engineering*, vol. 30, no. 10, p. e22356, 2020.
[6] M. O. Akinsolu *et al.*, "Machine learning-assisted antenna design optimization: A review and the state-of-the-art," in *2020 14th European Conference on Antennas and Propagation (EuCAP)*, 2020, pp. 1–5.
[7] B. A. F. Esmail and S. Koziel, "Design and optimization of metamaterial-based 5g millimeter wave antenna for gain enhancement," *IEEE Transactions on Circuits and Systems II: Express Briefs*, vol. 70, no. 9, pp. 3348–3352, 2023.
[8] J. Zhang *et al.*, "Automatic ai-driven design of mutual coupling reducing topologies for frequency reconfigurable antenna arrays," *IEEE Transactions on Antennas and Propagation*, vol. 69, no. 3, pp. 1831–1836, 2021.
[9] K. Fu *et al.*, "An efficient surrogate assisted particle swarm optimization for antenna synthesis," *IEEE Transactions on Antennas and Propagation*, vol. 70, no. 7, pp. 4977–4984, 2022.
[10] Q. Wu *et al.*, "Machine learning-assisted array synthesis using active base element modeling," *IEEE Transactions on Antennas and Propagation*, vol. 70, no. 7, pp. 5054–5065, 2022.
[11] S. Koziel *et al.*, "Low-cost and highly accurate behavioral modeling of antenna structures by means of knowledge-based domain-constrained deep learning surrogates," *IEEE Transactions on Antennas and Propagation*, vol. 71, no. 1, pp. 105–118, 2023.
[12] Q. Hua *et al.*, "A novel compact quadruple-band indoor base station antenna for 2g/3g/4g/5g systems," *IEEE Access*, vol. 7, pp. 151 350–151 358, 2019.
[13] B. Liu *et al.*, "An efficient method for complex antenna design based on a self adaptive surrogate model-assisted optimization technique," *IEEE Transactions on Antennas and Propagation*, vol. 69, no. 4, pp. 2302–2315, 2021.
[14] Y. Liu *et al.*, "An efficient method for antenna design based on a self-adaptive bayesian neural network-assisted global optimization technique," *IEEE Transactions on Antennas and Propagation*, vol. 70, no. 12, pp. 11 375–11 388, 2022.
[15] H. Aliakbarian *et al.*, "A digitally beam-steerable antenna array system for positioning-based tracking applications," *IEEE Antennas and Propagation Magazine*, vol. 55, no. 6, pp. 35–49, 2013.
[16] A. Ghadimi *et al.*, "A systematic approach for mutual coupling reduction between microstrip antennas using pixelization and binary optimization," *IEEE Antennas and Wireless Propagation Letters*, vol. 19, no. 12, pp. 2048–2052, 2020.
[17] J. Jayasinghe *et al.*, "Nonuniform overlapping method in designing microstrip patch antennas using genetic algorithm optimization," *International Journal of Antennas and Propagation*, vol. 2015, no. 805820, pp. 1–8, 2015.
[18] H.-W. Son and S.-H. Jeong, "Wideband rfid tag antenna for metallic surfaces using proximity-coupled feed," *IEEE Antennas and Wireless Propagation Letters*, vol. 10, pp. 377–380, 2011.